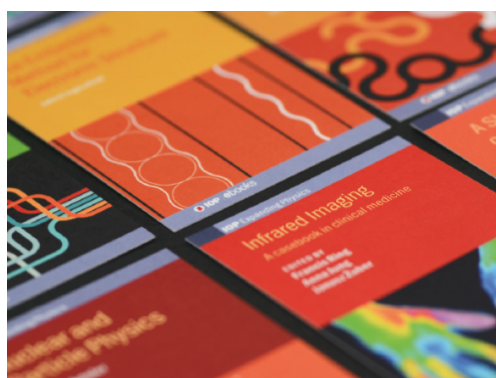


PAPER • OPEN ACCESS

## Superconductivity in Weyl Semimetal NbP: Bulk vs. Surface

To cite this article: M Baenitz *et al* 2019 *J. Phys.: Conf. Ser.* **1293** 012002

View the [article online](#) for updates and enhancements.



**IOP | ebooks™**

Bringing together innovative digital publishing with leading authors from the global scientific community.

Start exploring the collection—download the first chapter of every title for free.

# Superconductivity in Weyl Semimetal NbP: Bulk vs. Surface

M Baenitz<sup>1</sup>, M Schmidt<sup>1</sup>, V Suess<sup>1</sup>, C Felser<sup>1</sup> and K Lüders<sup>1,2</sup>

<sup>1</sup>Max-Planck-Institut für Chemische Physik fester Stoffe, Nöthnitzer Str. 40, 01187 Dresden, Germany

<sup>2</sup>Fachbereich Physik, Freie Universität Berlin, Arnimallee 14, 14195 Berlin, Germany

baenitz@cpfs.mpg.de

**Abstract.** Transition metal monpnictides belong to the new class of semimetals where the bulk properties are determined by the presence of pairs of nodes with different chirality formed by linear dispersive states in the k-space. Beside the anomaly in the bulk magnetotransport superconductivity is frequently found in some Weyl semimetals. We found signatures of superconductivity in ac and dc magnetization measurements of highly pure and stoichiometric NbP powder. We determined the lower and upper critical field and the Ginzburg-Landau parameter. The relative small superconducting volume fraction is related to either effect of finite grain size and/or surface superconductivity. The last mentioned may originate from either off stoichiometric (Nb-rich) surface layers or a strained surface with different electronic properties. Furthermore the intrinsic normal state susceptibility is determined taking into account a paramagnetic contribution of a few ppm of magnetic impurities.

## 1. Introduction

Niobium and its compounds play a major role in superconductivity including its applications to particle accelerators and superconducting magnets. Among the element superconductors niobium has with  $T_c = 9.5$  K the highest transition temperature and belongs to the three type-II superconductors. Many Nb compounds exhibit rather high transition temperatures, like NbN ( $T_c = 17$  K), NbC ( $T_c = 11.1$  K) or Nb<sub>3</sub>Ge which holds with  $T_c = 23.2$  K the record among the binary compounds.

The system NbN belongs to the Nb monpnictides. Within these systems NbP is one of the recently discovered Weyl semimetals, a novel state of topological quantum matter with exotic transport properties [1-4]. Some of the Weyl semimetals exhibit superconductivity (e.g. MoTe<sub>2</sub>) and there is a discussion if so-called type-II Weyl semimetals are the prime candidates for superconductivity [5, 6]. However, well prepared single crystals of NbP show no sign of superconductivity down to lowest temperatures [7]. Nonetheless there is strong evidence from various methods that Nb and even Ta based monpnictides are at the verge of superconductivity [8, 9]. It should also be mentioned that the magnetic counterparts MnP and CrAs show pressure induced superconductivity [10, 11].

On the other hand Nb based pnictide compounds with N, P or As show superconductivity. Well known is the system NbN which was already discovered in 1941. It shows a transition temperature of  $T_c = 17$  K and a penetration depth of the magnetic field of  $\lambda = 200$  nm. Recently it is also discussed for accelerator applications. Less known are the superconducting properties of NbP. Recently a transition temperature of  $T_c = 7.5$  K was published for NbP powder [12]. Some transition temperatures were published earlier for sputtered Nb-P samples in the composition range from 17 to 31 at.% P with  $T_c$ -



values from 6 K up to 7.5 K for 21 at.% P [13]. Nearly nothing is known about NbAs, the third compound in this group. Some experiments seem to indicate a superconducting transition at about 10 K [14].

In this publication results of superconducting properties of NbP powder are reported. Surprisingly superconductivity occurs after milling NbP single crystals to powder samples.

## 2. Experimental

Several powder samples of NbP are obtained by milling NbP single crystals the preparation and properties of which are described in ref. [3]. The largest NbP powder sample has a mass of about 500 mg (sample 1) and was used for detailed Nb- and P-NMR studies [15]. All powder samples are investigated by X-ray diffraction and lattice parameters obtained are in good agreement with the literature [16]. No sign of foreign phases could be found. It is remarkable that we found well defined de Haas-van Alphen oscillations even in powder samples (see supplemental material of ref. [17]). This we take as an evidence for the presence of rather pure single crystalline grains in the powder samples.

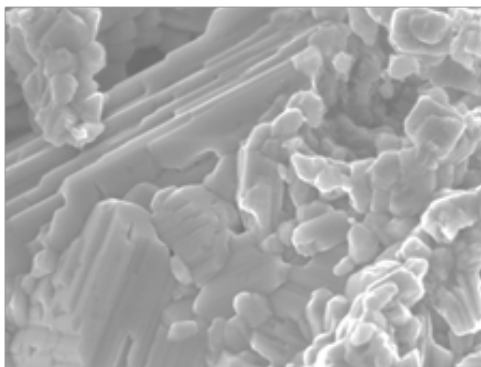
Zero field cooled (zfc), field cooled (fc), magnetization, and ac susceptibility measurements are performed by means of commercially available magnetometers (MPMS and PPMS, Quantum Design Inc.).

## 3. Results and discussion

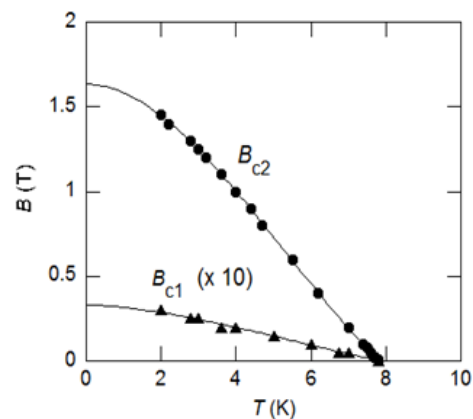
### 3.1. Structure and phase diagram

Figure 1 shows a scanning electron microscope (SEM) image of NbP powder. Different structure elements can be seen: small grains of about 100 nm size collected in larger conglomerates and larger blocs of parallel bars.

Figure 2 shows the superconducting phase diagram, i.e. the temperature dependence of the lower and upper critical field  $B_{c1}(T)$  and  $B_{c2}(T)$  determined from zfc-fc measurements and magnetization curves. The onset transition occurs at  $T_c = 7.8$  K. The phase diagram exhibits a clear type-II behavior without irreversibility line. The extrapolated values of the critical fields at  $T = 0$  are  $B_{c1}(0) = 34$  mT and  $B_{c2}(0) = 1.64$  T, respectively.



**Figure 1.** SEM image of NbP powder (scale:  $3 \times 2.25 \mu\text{m}$ )



**Figure 2.** Field-temperature diagram of NbP powder

### 3.2. Superconducting behavior

The upper critical field value at  $T = 0$ ,  $B_{c2}(0) = 1.64$  T, is slightly higher than the theoretical value of the WHH theory [18, 19],  $B^*_{c2}(0) = 1.5$  T, with the assumption of a clean limit and the resulting Maki parameter  $\alpha = 0.15$ . The reason for that might be a multi-phase grain structure of the sample or surface superconductivity. Following the expressions connecting the Ginzburg-Landau parameter  $\kappa$  with the

ratio of the two critical fields [20], leads to a value of  $\kappa = 6.96$ . This  $\kappa$ -value clearly indicates superconducting type-II behavior and is of order of other Nb compounds. It is considerably larger than that of pure niobium ( $\kappa_{\text{Nb}} = 0.8$ ) but well below  $\kappa = 40$ , the value of the A-15 compound  $\text{Nb}_3\text{Sn}$ .

The magnetic penetration depth  $\lambda(0)$  is determined from  $B_{c2}(0)$  via the Ginzburg-Landau coherence length  $\xi_{\text{GL}}(0)$  using the relations  $\lambda = \kappa \cdot \xi$  and  $\xi^2 = \Phi_0 / 2\pi B_{c2}$  ( $\Phi_0 = \text{flux quantum} = h/2e$ ). With  $\kappa = 6.96$  and  $\xi_{\text{GL}}(0) = 14.2$  nm the penetration depth results to  $\lambda_{\text{GL}}(0) = 98.8$  nm. Figure 3 shows zfc and fc curves for two magnetic fields. Plotted is the volume susceptibility which allows the determination of the superconducting volume fraction. For sample 2 which is shown in the figure it results to 6.2 %. Due to the presence of small grains (with dimensions in the order of the penetration depth) the determined fraction underestimates the real superconducting volume. An analysis of magnetization curves leads to the same value. As an example the magnetization curve for  $T = 2$  K of sample 2 is plotted in Figure 4.

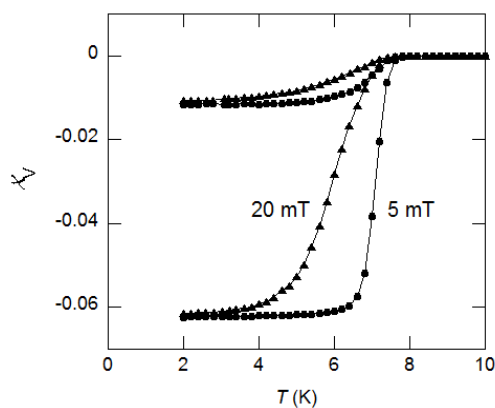


**Figure 3.** Zfc and fc transition curves in two magnetic fields. Plotted is the volume susceptibility calculated from the measured magnetic moment.

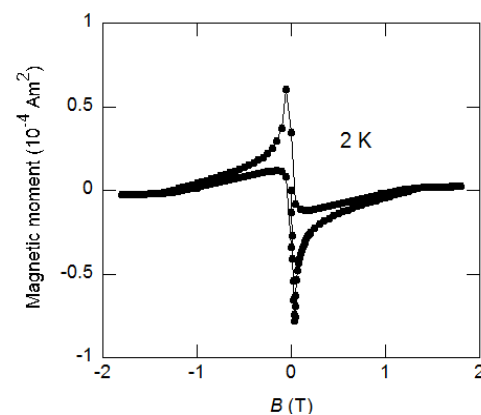


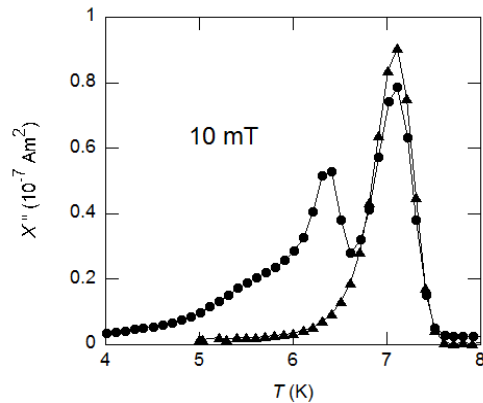
**Figure 4.** Magnetization curve of NbP powder obtained at a temperature of 2 K. Here the magnetic moment is plotted against the magnetic field  $B$ .

### 3.3. Ac susceptibility

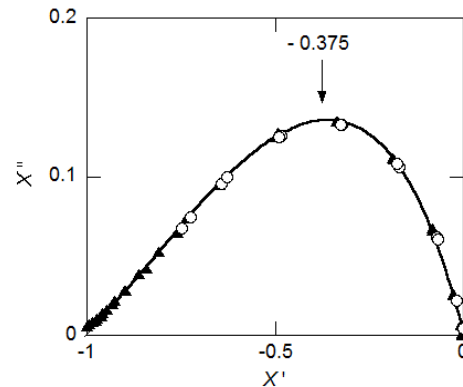
In order to get more information about the vortex dynamics ac susceptibility measurements are performed. The temperature dependence of the real and imaginary parts of the ac susceptibility,  $\chi'$  and  $\chi''$ , was recorded starting at low temperatures up to temperatures well above the transition temperature and back again. Magnetic fields are applied up to  $B = 40$  mT. Frequency and ac field amplitude were fixed to 0.1 kHz and 10 mT, respectively. The real parts are in rather good agreement with the respective zfc transition curves.

Figure 5 shows a comparison of imaginary parts of the ac susceptibility for two samples. In the case of sample 1 only one peak occurs starting at the transition temperature of  $T_c = 7.6$  K and passing its maximum at  $T = 7.1$  K. For sample 2, however, a second peak occurs at lower temperature with its maximum at  $T = 6.4$  K. It originates most likely from intergranular superconducting contacts between the grains.

In Figure 6 the imaginary parts of the ac susceptibility are plotted against their real parts. The peak height of  $\chi''$  is about 14 % of the maximum values of  $\chi'$ . This kind of plot can be compared with theoretical predictions [21] based either on Bean's critical state model [22] or other models based on diffusive motion of the flux lines for example [23]. In our case, however, the curves are in excellent agreement with the prediction of the critical state model with a maximum at  $\chi' = -0.375$ .



**Figure 5.** Comparison of the imaginary parts  $\chi''$  of the ac susceptibility for sample 1 (triangles) and 2 (circles) obtained in a magnetic field of 10 mT



**Figure 6.** Imaginary parts  $\chi''$  plotted against their real parts  $\chi'$  of the ac susceptibility at a magnetic field of 10 mT (sample 1 triangles and 2 open circles). The axes are normalized to the lowest value of  $\chi'$ .

### 3.4. Magnetic behavior

Figure 7 shows as an example the fc curve of sample 1 in an applied magnetic field of  $B = 0.25$  T. In order to investigate the magnetic properties of NbP powder at first the temperature independent contribution was determined. The temperature dependence of the non-superconducting part of the curve evidences the presence of i) a Curie-like paramagnetism and ii) a temperature and field independent diamagnetic contribution  $\chi_{\text{Dia}}$ . A  $1/T$ -extrapolation of the non-superconducting part to infinite temperature leads to the diamagnetic contribution. It is represented by the horizontal line in Figure 7 whereas the Curie-like contribution is represented by the curved line. The corresponding diamagnetic volume susceptibility is  $\chi_{\text{Dia}} = -4.0 \cdot 10^{-5}$  ( $-6.1 \cdot 10^{-5}$  emu/mol). The diamagnetic core contribution for NbP is estimated in ref. [16] to be  $-7.4 \cdot 10^{-5}$  emu/mol. This suggests a small positive intrinsic powder susceptibility for NbP of  $+1.3 \cdot 10^{-5}$  emu/mol due to a small but finite number of carriers.

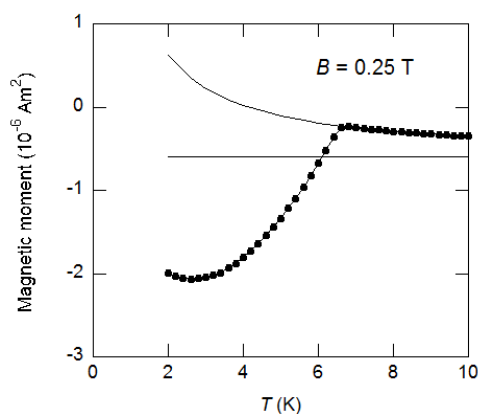


**Figure 7.** Diamagnetic (horizontal line) and paramagnetic (upper  $1/T$ -line) contributions extrapolated from the non-superconducting part of an fc curve at the magnetic field  $B = 0.25$  T (sample 1)

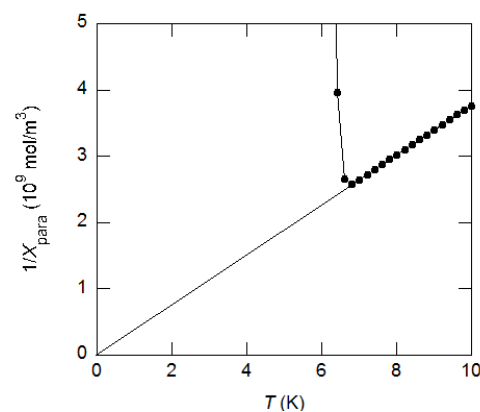


**Figure 8.** Plot of the same data for the determination of the paramagnetic moment

To determine the paramagnetic effective Curie moment  $\mu$  the reciprocal paramagnetic volume susceptibility is plotted against the temperature (Figure 8). We obtain a value of  $\mu = 0.041 \mu_B$  ( $\mu_B =$  Bohr magneton). Comparable values were found for the other samples as plotted in Table 1. This magnetism originate probably from a very tiny amount (about 60 ppm) of magnetic ions (probably Fe or Ni) which is in the specified purity range of commercially available elements used for the synthesis (see discussion in ref. [17]).

**Table 1.** Superconductivity and magnetic properties of NbP powder ( $\mu_B =$  Bohr magneton =  $9.274 \cdot 10^{-24}$  Am<sup>2</sup>)

Sample	1	2	3
$T_c$ (K)	7.6	7.8; 6.7	8.7; 7.2
$B_{c2}(0)$ (T)		1.64	
$B_{c1}(0)$ (T)		0.034	
superconducting volume fraction (%)	0.4	6.2	0.02
diamagnetic volume susceptibility	$-3.5 \cdot 10^{-5}$	$-4.0 \cdot 10^{-5}$	from $-2.1 \cdot 10^{-5}$ to $-6.1 \cdot 10^{-5}$
paramagnetic moment	$0.041 \mu_B$	$0.045 \mu_B$	$0.043 \mu_B$

## Conclusions

Powder samples of highly pure and stoichiometric NbP exhibit superconductivity with transition temperatures between 6 and 9 K in accordance with other published values for Nb-P compounds. The superconducting phase diagram shows a clear type-II behavior with a Ginzburg-Landau parameter of about  $\kappa = 7$  and a penetration depth of about  $\lambda_{GL}(0) = 100$  nm. Although the transition temperatures are similar to those of pure Nb the behavior in magnetic fields is quite different. The Ginzburg-Landau parameter as well as the upper critical field is larger by a factor of 6 to 7. The relatively small superconducting volume fraction of a few percent might be due to grain size effects. It might be speculated that the powder grains are strained and the system converts into a type-II Weyl semimetal for which superconductivity is more likely. A more detailed study is required to support this scenario.

## Acknowledgments

The authors would like to thank H. Rave for her support in the experiments. We thank P. Werner (MPI of Microstructure Physics, Halle) for providing the SEM picture. One of us (KL) would like to thank C. Felser and A.P. Mackenzie for their kind hospitality and the possibility of doing research at the MPI-CPfS.

## References

- [1] Weng H, Fang C, Fang Z, Bernevig B A and Dai X 2015 *Phys. Rev. X* **5** 011029
- [2] Sun Y, Wu S-C and Yan B 2015 *Phys. Rev. B* **92** 115428
- [3] Shekhar C, Nayak A K, Sun Y, Schmidt M, Nicklas M, Leermakers I, Zeitler U, Skourski Y, Wosnitza J, Liu Z, Chen Y, Schnelle W, Borrmann H, Grin Y, Felser C and Yan B 2015 *Nature Physics* **11** 645
- [4] Klotz J, Wu S-C, Shekhar C, Sun Y, Schmidt M, Nicklas M, Baenitz M, Uhlarz M, Wosnitza J, Felser C and Yan B 2016 *Phys. Rev. B* **93** 121105
- [5] Alidoust M, Halterman K and Zyuzin A A 2017 *Phys. Rev. B* **95** 155124
- [6] Rosenstein B, Shapiro B Y, Li D and Shapiro I 2018 *Phys. Rev. B* **97** 144510

- [7] Stockert U, dos Reis R D, Ajeesh M O, Watzman S J, Schmidt M, Shekhar C, Heremans J P, Felser C, Baenitz M and Nicklas M 2017 *J. Phys.: Condens. Matter* **29** 325701
- [8] Bachmann M D, Nair N, Flicker F, Ilan R, Meng T, Ghimire N J, Bauer E D, Ronning F, Analytis J G and Moll P J W 2017 *Sci. Adv.* **3** e160298
- [9] Aggarwal L, Gayen S, Das S, Kumar R, Süß V, Felser C, Shekhar C and Sheet G 2016 *Nature Communications* **8** 13974
- [10] Cheng J G, Matsubayashi K, Wu W, Sun J P, Lin F K, Luo J L and Uwatoko Y 2015 *Phys. Rev. Lett.* **114** 117001
- [11] Wu W, Cheng J, Matsubayashi K, Kong P, Lin F, Jin C, Wang N, Uwatoko Y and Luo J 2014 *Nature Communications* **5** 5508
- [12] Kumar P, Sudesh and Patnaik S 2016 *AIP Conf. Proc.* **1731** 140063
- [13] Johnson G R and Douglass D H 1974 *Journal of Low Temperature Physics* **14** 575
- [14] Baenitz M, to be published
- [15] Yasuoka H et al., to be published
- [16] Xu J, Greenblatt M, Emge T, Höhn P, Hughbanks T and Tian Y 1996 *Inorg. Chem.* **35** 845
- [17] Yasuoka H, Kubo T, Kishimoto Y, Kasinathan D, Schmidt M, Yan B, Zhang Y, Tou H, Felser C, Mackenzie A P and Baenitz M 2017 *Phys. Rev. Lett.* **118** 236403
- [18] Helfand E and Werthamer N R 1966 *Phys. Rev.* **147** 288
- [19] Werthamer N R, Helfand E and Hohenberg P C 1966 *Phys. Rev.* **147** 295
- [20] Brandt E H 2003 *Phys. Rev. B* **68** 054506
- [21] Ling X and Budnick J I 1991 *Magnetic Susceptibility of Superconductors and other Spin Systems*, ed R A Hein *et al* (New York and London: Plenum Press) p 377
- [22] Bean C P 1964 *Rev. Mod. Phys.* **34** 31
- [23] Khoder A F and Couach M 1991 *Magnetic Susceptibility of Superconductors and other Spin Systems*, ed R A Hein *et al* (New York and London: Plenum Press) p 213